Vol 10 No 3, March 2001
1009-1963/2001/10(03)/0206-08

Chinese Physics

© 2001 Chin. Phys. Soc.
and IOP Publishing Ltd

INTERFERENCE EFFECTS IN DIFFERENT FIFTH-ORDER POLARIZATIONS WITH BROADBAND NOISY LIGHT*

ZHANG YAN-PENG(张彦鹏)[a)b)], WU HONG-CAI(吴洪才)[)], LU KE-QING(卢克清)[a)],
HOU XUN(侯 洵) and CID B. DE ARAÚJO[c)]

[a)] *Department of Electronic Science and Technology, Xi'an Jiaotong University, Xi'an 710049, China*

[b)] *State Key Laboratory of Transient Optics and Technology, Xi'an Institute of Optics and Precision Mechanics, Chinese Academy of Sciences, Xi'an 710068, China*

[c)] *Departamento de Física, Universidade Federal de Pernambuco, 50670-901 Recife, PE, Brazil*

(Received 15 July 2000)

Based on the second-order coherence function, we have studied a phase-conjugate ultrafast modulation spectroscopy due to the interference between the fifth- and fifth-order optical polarizations in cascade three-level Doppler-broadened system. It is found that the temporal behaviour of the beat signal depends on the stochastic properties of the lasers and the transverse relaxation rate of the transition. The beat signal depends on the second-order coherence function, which is determined by the laser line shape. Since different stochastic models of the laser field only affect higher than second-order coherence functions, they have little influence on the general temporal modulation behaviour of the beat signal. The cases that pump beams have either narrow band or broadband linewidth are considered and it has been found that for both cases the overall accuracy for the energy-level difference measurement is determined by the homogeneous linewidths of the optical transitions. Finally, the spatial modulation behaviour of the beat signal has also been discussed.

Keywords: interference, six-wave mixing, two-photon
PACC: 4265, 3290

I. INTRODUCTION

For many years, nonlinear optical spectroscopies have been a standard tool in the investigation of material dynamics. Currently, time-resolved nonlinear optical techniques, which employ ultrashort light pulses, are ubiquitous in many areas of physical, chemical, biological and medical research. While the richness of information generally increases with increasing order in the perturbing electric fields, so does the difficulty of performing and interpreting the experiment. Higher-order time-resolved nonlinear optical processes can often be obscured by sequential lower order processes that compete with the direct event, and give similar time domain behaviour, though they probe different dynamics. Hence, for isotropic media, the vast majority of such nonlinear spectroscopies are third-order in the electric field. Polarization beat is a phenomenon that results from the interference between the macroscopic polarizations excited in a nonlinear material. The radiation beams generated by these polarizations interfere with each other, producing a modulation of the signal intensity emitted by the sample. This effect is qualitatively different from quantum beats, which originate from interference between wavefunction amplitudes. Polarization beats have attracted considerable attention recently. DeBeer *et al.*[1] performed the first ultrafast modulation spectroscopy (UMS) experiment in sodium vapour. The beating signal exhibits 1.9ps modulation corresponding to the sodium D-line splitting when the time delay between two double-frequency pump beams increases. It is worth mentioning that the UMS proposed by DeBeer *et al.* is not Doppler-free for narrowband laser excitation when beams 1 and 2 are overlapped temporally. In this case, the modulation frequency equals $\omega_2 - \omega_1$, and the four-wave mixing (FWM) with self-diffraction geometry cannot provide a Doppler-free spectrum. Fu *et al.*[2] then analysed the UMS with phase-conjugate geometry in a Doppler-broadened system. They found that a Doppler-free precision in the measurement of the energy-level splitting could be achieved. In this case, when pulse laser beams 1 and 2 are separated temporally, then before the application of beam 2, the polarization exhibits free evolution. As a result, the modulation frequency is directly related to the energy level of the system, no

*Project supported by the National Natural Science Foundation of China (Grant No.69978019) and the State Key Laboratory Foundation of Transient Optics Technology (Grant No.YAK20006).

matter whether the pump beams have a narrow-band or a broadband linewidth. The UMS technique has also been applied to a cascade three-level system.[3] This phenomenon was explained as the third-order polarization interference between two different channels. Later, Ma *et al.*[4] developed a polarization beat interferometry to measure the phase of the third-order susceptibilities of the Cd(S,Se)-doped glasses. They also observed interference between the third- and the fifth-order polarization in semiconductor doped glasses.[5]

The atomic response to Markovian stochastic optical fields is now largely well understood. Methods exist to calculate the first-order moments of the atomic density matrix elements for a wide variety of field statistics, including phase-diffusing fields,[6,7] phase-diffusing fields with coloured noise, chaotic fields,[3,8−12] real Gaussian fields[13,14] and phase jump fields. These methods are valid for arbitrary field strengths and bandwidths, and could properly account for all orders of electric-field correlations. It is generally straightforward to extend these methods to include products of density elements, useful for calculating observables, such as the variance of fluorescence intensity or the intensity of FWM signals.[15] In these works, coloured noise models, which incorporate a memory into the process and are non-Markovian, can be reduced to Markovian processes by an extension of the number of dimensions in the problem. In this paper, we assume that the laser sources are chaotic fields. A chaotic field, which is used to describe a multimode laser source, is characterized by the fluctuation of both the amplitude and the phase of the field. Another commonly used stochastic model is the phase-diffusion model, which is used to describe an amplitude-stabilized laser source. This model assumes that the amplitude of the laser field is constant, while its phase fluctuates as a random process caused by spontaneous emission. We present a second-order coherence function theory to elucidate the physics of the basic features of the nonlinear effect of fifth-order on polarization beats in a cascade three-level system. The beat signal depends on the second-order coherence function, which is determined by the laser line shape. Since different stochastic models for the laser field only affect higher than second-order coherence functions,[3,10,11] they have little influence on the general temporal modulation behaviour of the beat signal.

In this paper, we report on the fifth-order femtosecond polarization beats induced by the fifth-order susceptibility in a cascade three-level Doppler-broadened system. The cases in which the pump beams have either a narrow-band or a broadband linewidth are considered, and it is found that the beat signal oscillates not only temporally but also spatially. If the fifth-order polarization beat is employed for the energy-level difference measurement, there are advantages that the energy-level difference between states can be separated widely, and a Doppler-free precision in the measurement can be achieved. We have also investigated the relationship between the fifth-order polarization beats and other Doppler-free techniques in frequency and in time domains. It is found that the fifth-order polarization beat is closely related to the Doppler-free saturated absorption spectroscopy (or two-photon absorption spectroscopy with a resonant intermediate state) and the three-pulse stimulated photon echo (or sum-frequency trilevel photon-echo) when the pump beams are of narrow-band and broadband linewidths,[2] respectively. However, it possesses the main advantages of these techniques in the frequency and in the time domains.

II. BASIC THEORY

Fifth-order polarization beats in a cascade three-level system (FPBCTS) is a polarization beat phenomenon originating from the interference between the one-photon six-wave mixing and the two-photon six-wave mixing processes. Let us consider a cascade three-level atomic system (Fig.1) with a ground state $|0\rangle$, an intermediate state $|1\rangle$ and an excited state $|2\rangle$. The states between $|0\rangle$ and $|1\rangle$ and between $|1\rangle$ and $|2\rangle$ are coupled by dipolar transition with resonant frequencies Ω_1 and Ω_2, respectively, while the states between $|0\rangle$ and $|2\rangle$ are dipolar forbidden. We consider, in this cascade three-level system, double-frequency time-delay four-wave mixing and six-wave mixing (SWM) polarization beats in which beams 1 and 2 consist of two-frequency components ω_1 and ω_2, while beam 3 has a frequency ω_3 (Fig.2). All the incident beams are linearly polarized in the same direction. The beat signal has the same polarization as the incident beam, propagating along a direction almost opposite to that of beam 2. It could be detected by a photodiode. We assume that $\omega_1 \approx \Omega_1 (\omega_3 \approx \Omega_1)$ and $\omega_2 \approx \Omega_2$, hence ω_1 and ω_2 will drive the transitions from $|0\rangle$ to $|1\rangle$ and from $|1\rangle$ to $|2\rangle$, respectively. In third-order polarization beats,[3] there are two processes involved in this double-frequency time-delay FWM. Firstly, the ω_1 frequency component of beams 1 and 2 induces population gratings of states $|0\rangle$ and $|1\rangle$, which are probed by beam 3 frequency

ω_3. This is a one-photon resonant degenerate FWM and the signal (beam 4) has a frequency ω_3. Secondly, beam 3 and the ω_2 frequency component of beam 1 induce the coherence between $|0\rangle$ and $|2\rangle$ by two-photon transition, which is then probed by the ω_2 frequency component of beam 2. This is a two-photon nondegenerate FWM with a resonant intermediate state, and the frequency of the signal (beam 4) equals ω_3. We are interested in the dependence of the beat signal intensity on the relative time delay between beams 1 and 2. One-photon and two-photon FWM signals (beam 4) with frequency ω_3 will be emitted along the directions $\boldsymbol{k}_1 - \boldsymbol{k}_1 + \boldsymbol{k}_3$ and $\boldsymbol{k}_2 - \boldsymbol{k}_2' + \boldsymbol{k}_3$, respectively. In the fifth-order polarization beats, one-photon degenerate SWM signals (beam 5) with frequency ω_3 will be emitted along the direction $2\boldsymbol{k}_1 - 2\boldsymbol{k}_1' + \boldsymbol{k}_3$, while two-photon nondegenerate SWM signals (beam 5) with frequency ω_3 will be emitted along the directions $2\boldsymbol{k}_2 - 2\boldsymbol{k}_2' + \boldsymbol{k}_3$ and $\boldsymbol{k}_3 + \boldsymbol{k}_1 - \boldsymbol{k}_1' + \boldsymbol{k}_2 - \boldsymbol{k}_2'$. In the phase-conjugation geometry, beams 4 and 5 have a small angle between them.

The direct fifth-order polarization beat processes can often be obscured by cascaded or sequential lower-order processes that compete with the direct event, and they give similar time-domain behaviour though they probe different dynamics.[5,16] The one-order diffraction signal (beam 4) is contributed primarily by the third-order nonlinear polarization, whereas the second-order diffraction signal (beam 5) may include contributions from the fifth-order nonlinear polarization and the cascade processes due to the third-order nonlinear polarization. Let us assume here that the cascade contribution is negligible as compared to that of direct fifth-order nonlinearity. If the FWM signals (beam 4) are blocked, the SWM signals can be detected along the direction of beam 5.

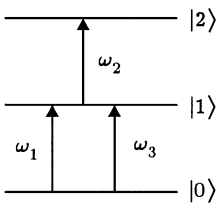


Fig.1. Cascade three-level configuration to be treated by FPBCTS.

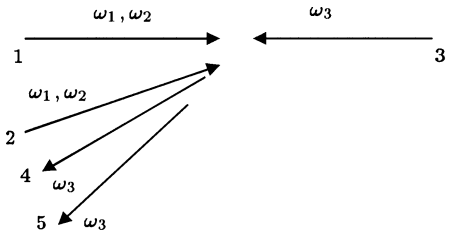


Fig.2. Schematic diagram of the geometry of FPBCTS.

The complex electric fields of beam 1, E_{p1}, and beam 2, E_{p2}, can be written as

$$\begin{aligned} E_{p1} =& A_1(\boldsymbol{r},t)\exp(-\mathrm{i}\omega_1 t) + A_2(\boldsymbol{r},t)\exp(-\mathrm{i}\omega_2 t) \\ =& \varepsilon_1 u_1(t)\exp[\mathrm{i}(\boldsymbol{k}\cdot\boldsymbol{r} - \omega_1 t)] \\ &+ \varepsilon_2 u_2(t)\exp[\mathrm{i}(\boldsymbol{k}_2\cdot\boldsymbol{r} - \omega_2 t)], \end{aligned}$$

$$\begin{aligned} E_{p2} =& A_1'(\boldsymbol{r},t)\exp(-\mathrm{i}\omega_1 t) + A_2'(\boldsymbol{r},t)\exp(-\mathrm{i}\omega_2 t) \\ =& \varepsilon_1' u_1(t-\tau)\exp[\mathrm{i}(\boldsymbol{k}'\cdot\boldsymbol{r} - \omega_1 t + \omega_1\tau)] \\ &+ \varepsilon_2' u_2(t-\tau)\exp[\mathrm{i}(\boldsymbol{k}_2'\cdot\boldsymbol{r} - \omega_2 t + \omega_2\tau)]. \end{aligned}$$

Here, ε_i, $\boldsymbol{k}_i(\varepsilon_i', \boldsymbol{k}_i')$ are the constant field amplitude and the wave vector of the ω_i component in beam 1 (beam 2), respectively; $u_i(t)$ is a dimensionless statistical factor that contains phase and amplitude fluctuations. We assume that the ω_1 (ω_2) component of E_{p1} and E_{p2} comes from a single laser source and τ is the time delay of beam 2 with respect to beam 1. On the other hand, beam 3 is assumed to be a quasi-monochromatic light. The complex electric fields of beam 3 can be written as

$$E_{p3} = A_3(\boldsymbol{r},t)\exp(-\mathrm{i}\omega_3 t) = \varepsilon_3\exp[\mathrm{i}(\boldsymbol{k}_3\cdot\boldsymbol{r} - \omega_3 t)].$$

Here, ω_3, ε_3, and $\boldsymbol{k}_3$ are the frequency, the field amplitude and the wave vector of the field, respectively.

We employ perturbation theory to calculate the density matrix elements. The third-order off-diagonal density matrix element $\rho_{10}^{(3)}$, which has wave vectors $\boldsymbol{k}_1 - \boldsymbol{k}_1' + \boldsymbol{k}_3$ and $\boldsymbol{k}_2 - \boldsymbol{k}_2' + \boldsymbol{k}_3$ responsible for the FWM signal in the cascade three-level system, can be calculated by following the perturbation channels[3]:

(a) $\rho_{00}^{(0)} \xrightarrow{A_1} \rho_{10}^{(1)} \xrightarrow{(A_1')^*} \rho_{00}^{(2)} \xrightarrow{A_3} \rho_{10}^{(3)}$,
(b) $\rho_{00}^{(0)} \xrightarrow{(A_1')^*} (\rho_{10}^{(1)})^* \xrightarrow{A_1} \rho_{00}^{(2)} \xrightarrow{A_3} \rho_{10}^{(3)}$,
(c) $\rho_{00}^{(0)} \xrightarrow{A_1} \rho_{10}^{(1)} \xrightarrow{(A_1')^*} \rho_{11}^{(2)} \xrightarrow{A_3} \rho_{10}^{(3)}$,
(d) $\rho_{00}^{(0)} \xrightarrow{(A_1')^*} (\rho_{10}^{(1)})^* \xrightarrow{A_1} \rho_{11}^{(2)} \xrightarrow{A_3} \rho_{10}^{(3)}$,
(e) $\rho_{00}^{(0)} \xrightarrow{A_3} \rho_{10}^{(1)} \xrightarrow{A_2} \rho_{20}^{(2)} \xrightarrow{(A_2')^*} \rho_{10}^{(3)}$,

Chains (a)–(d) correspond to the one-photon resonant degenerate FWM processes, while chain (e) corresponds to the two-photon resonant nondegenerate FWM processes.

On the other hand, the fifth-order off-diagonal density matrix element $\rho_{10}^{(5)}$, which has wave vectors $2\boldsymbol{k}_1-2\boldsymbol{k}_1'+\boldsymbol{k}_3$, $2\boldsymbol{k}_2-2\boldsymbol{k}_2'+\boldsymbol{k}_3$ and $\boldsymbol{k}_3+\boldsymbol{k}_1-\boldsymbol{k}_1'+\boldsymbol{k}_2-\boldsymbol{k}_2'$ responsible for the SWM signal in the cascade three-level system, can be calculated by the following perturbation channels:

(I) $\rho_{00}^{(0)} \xrightarrow{A_1} \rho_{10}^{(1)} \xrightarrow{(A_1')^*} \rho_{00}^{(2)} \xrightarrow{A_1} \rho_{10}^{(3)} \xrightarrow{(A_1')^*} \rho_{00}^{(4)} \xrightarrow{A_3} \rho_{10}^{(5)}$,

(II) $\rho_{00}^{(0)} \xrightarrow{A_1} \rho_{10}^{(1)} \xrightarrow{(A_1')^*} \rho_{11}^{(2)} \xrightarrow{A_1} \rho_{10}^{(3)} \xrightarrow{(A_1')^*} \rho_{11}^{(4)} \xrightarrow{A_3} \rho_{10}^{(5)}$,

(III) $\rho_{00}^{(0)} \xrightarrow{A_1} \rho_{10}^{(1)} \xrightarrow{(A_1')^*} \rho_{11}^{(2)} \xrightarrow{A_2} \rho_{21}^{(3)} \xrightarrow{(A_2')^*} \rho_{11}^{(4)} \xrightarrow{A_3} \rho_{10}^{(5)}$,

(IV) $\rho_{00}^{(0)} \xrightarrow{A_3} \rho_{10}^{(1)} \xrightarrow{A_2} \rho_{20}^{(2)} \xrightarrow{(A_2')^*} \rho_{10}^{(3)} \xrightarrow{A_2} \rho_{20}^{(4)} \xrightarrow{(A_2')^*} \rho_{10}^{(5)}$,

(V) $\rho_{00}^{(0)} \xrightarrow{A_3} \rho_{10}^{(1)} \xrightarrow{A_2} \rho_{20}^{(2)} \xrightarrow{(A_1')^*} \rho_{21}^{(3)} \xrightarrow{(A_2')^*} \rho_{11}^{(4)} \xrightarrow{A_1} \rho_{10}^{(5)}$,

(VI) $\rho_{00}^{(0)} \xrightarrow{A_3} \rho_{10}^{(1)} \xrightarrow{A_2} \rho_{20}^{(2)} \xrightarrow{(A_1')^*} \rho_{21}^{(3)} \xrightarrow{A_1} \rho_{20}^{(4)} \xrightarrow{(A_2')^*} \rho_{10}^{(5)}$.

In perturbation chains (I), (II), (III), we note that the role of complex amplitudes A_1 and $(A_1')^*$, complex amplitudes A_2 and $(A_2')^*$ can be interchangeable here, respectively. The total perturbation chains of the SWM signal are 15. Chains (I), (II) correspond to the one-photon resonant degenerate SWM, while (III)–(VI) correspond to the two-photon resonant non-degenerate SWM. We are only interested in the beat signal with modulation frequency $\omega_2-\omega_1$, so there are two beating approaches (I), (II), (III), (V), (VI) and (III), (IV), (V), (VI).

The SWM signal is related to the fifth-order off-diagonal density matrix element $\rho_{10}^{(5)}$. It can be calculated by the perturbation chains (I)–(VI).

The nonlinear polarization $P^{(5)}$ responsible for the phase-conjugate SWM signal is given by averaging over the velocity distribution function $w(\boldsymbol{v})$. Thus

$$P^{(5)} = N\mu_1 \int_{-\infty}^{+\infty} \mathrm{d}\boldsymbol{v} w(\boldsymbol{v}) \rho_{10}^{(5)}(\boldsymbol{v}).$$

Here, $\boldsymbol{v}$ is the atomic velocity, N the density of atoms. For a Doppler-broadened atomic system, we have

$$w(\boldsymbol{v}) = \frac{1}{\sqrt{\pi}u} \exp[-(\boldsymbol{v}/u)^2].$$

The SWM signal is proportional to the average of the absolute square of $P^{(5)}$ over the random variable of the stochastic process $< |P^{(5)}|^2 >$, which involves eighth-order coherence function of $u_i(t)$ in phase-conjugation geometry. While the SWM signal intensity in DeBeer's self-diffraction geometry is related to the tenth-order coherence function of the incident fields. We assume that beam 1 (beam 2) is a multimode thermal source, which can be described as a chaotic model. In this case, $u_i(t)$ has Gaussian statistics characteristics.[17]

In this paper we are only interested in the τ-dependent part of the signal. The SWM signal intensity can be well approximated by the absolute square of the stochastic average of the polarization $| < P^{(5)} > |^2$, which involves a second-order function of $u_i(t)$. Here we develop a second-order function theory to study the effect of laser coherence. This theory is valid when we are only interested in the τ-dependent part of the beating signal. Furthermore, assuming that beam 1 (beam 2) has a Lorentzian line shape, then we have $< u_i(t_1)u_i^*(t_2) > = \exp(-\alpha_i|t_1-t_2|), (i=1,2)$, here $\alpha_i = \frac{1}{2}\delta\omega_i$ with $\delta\omega_i$ being the linewidth of the laser with frequency ω_i.

We first consider the case that beams 1 and 2 are narrow band, so that $\alpha_1 \ll \Gamma_{10}$ and $\alpha_2 \ll \Gamma_{20}$. For simplicity, here we neglect the Doppler effect. Performing the tedious integration in the first beating approach, the beat signal intensity then becomes

$$\begin{aligned} I(\tau) \propto\ & |B_1|^2 \exp(-4\alpha_1|\tau|) \\ & + |\eta B_2|^2 \exp[-2(\alpha_1+\alpha_2)|\tau|] \\ & + \exp[-(3\alpha_1+\alpha_2)|\tau|] \\ & \cdot \{\eta B_1^* B_2 \exp[-\mathrm{i}\Delta\boldsymbol{k}\cdot\boldsymbol{r} - \mathrm{i}(\omega_2-\omega_1)\tau] \\ & + \eta^* B_1 B_2^* \exp[\mathrm{i}\Delta\boldsymbol{k}\cdot\boldsymbol{r} + \mathrm{i}(\omega_2-\omega_1)\tau]\}. \end{aligned} \quad (1)$$

In the second beating approach, the beat signal intensity then becomes

$$\begin{aligned} I(\tau) \propto\ & |B_2|^2 \exp[-2(\alpha_1+\alpha_2)|\tau|] \\ & + |\eta B_3|^2 \exp(-4\alpha_2|\tau|) \\ & + \exp[-(\alpha_1+3\alpha_2)|\tau|] \\ & \cdot \{\eta B_2^* B_3 \exp[-\mathrm{i}\Delta\boldsymbol{k}\cdot\boldsymbol{r} - \mathrm{i}(\omega_2-\omega_1)\tau] \\ & + \eta^* B_2 B_3^* \exp[\mathrm{i}\Delta\boldsymbol{k}\cdot\boldsymbol{r} + \mathrm{i}(\omega_2-\omega_1)\tau]\}. \end{aligned} \quad (2)$$

Here B_1, B_2 and B_3 depending on the laser linewidths, frequency detuning and relaxation rate of the transition are τ-independent constants; $\eta = \frac{\mu_3^2}{\mu_1^2}\left[\frac{\varepsilon_2(\varepsilon_2')^*}{\varepsilon_1(\varepsilon_1')^*}\right]$, where $\mu_1(\mu_3)$ is the dipole-moment matrix element between $|0\rangle$ and $|1\rangle$ ($|1\rangle$ and $|2\rangle$); Γ_0 (Γ_1) is the population relaxation rate of state $|0\rangle$ ($|1\rangle$); Γ_{21} and $\Gamma_{10}(\Gamma_{20})$ are the transverse relaxation rates of the coherence between states $|1\rangle$ and $|2\rangle$ and between $|0\rangle$ and $|1\rangle(|2\rangle)$, respectively; $\Delta_1 = \Omega_1-\omega_1, \Delta_2 = \Omega_2-\omega_2, \Delta_3 = \Omega_3-\omega_3$.

Equations (1) and (2) indicate that the signal intensity oscillates not only temporally with a period $\omega_2-\omega_1$, but also spatially with a period $2\pi/\Delta k$ along

the direction $\Delta\boldsymbol{k} = (\boldsymbol{k}_1 - \boldsymbol{k}_1') - (\boldsymbol{k}_2 - \boldsymbol{k}_2')$, which is almost perpendicular to the propagation direction of the beat signal. Here $\Delta\boldsymbol{k} \approx 2\pi|\lambda_1 - \lambda_2|\theta/\lambda_2\lambda_1, \theta$ is the angle between beams 1 and 2. Physically, the polarization-beat model assumes that both the pump beams are plane waves. Therefore, one-photon SWM signals, which propagate along $\boldsymbol{k}_{s_1} = 2\boldsymbol{k}_1 - 2\boldsymbol{k}_1' + \boldsymbol{k}_3$, are plane waves also. Two-photon SWM signals, which propagate along $\boldsymbol{k}_{s_2} = \boldsymbol{k}_3 + \boldsymbol{k}_1 - \boldsymbol{k}_1' + \boldsymbol{k}_2 - \boldsymbol{k}_2'$ or $\boldsymbol{k}_{s_3} = 2\boldsymbol{k}_2 - 2\boldsymbol{k}_2' + \boldsymbol{k}_3$, are plane waves also. Since one- and two-photon SWM signals (i.e., $\boldsymbol{k}_{s_1}$ and $\boldsymbol{k}_{s_2}$ belong to the first beating approach) or two two-photon SWM signals (i.e., $\boldsymbol{k}_{s_2}$ and $\boldsymbol{k}_{s_3}$ belong to the second beating approach) propagate along a slightly different direction, the interference between them leads to the spatial oscillation. Equations (1) and (2) also indicate that beat signal modulates with a damping rate $3\alpha_1 + \alpha_2$ and $\alpha_1 + 3\alpha_2$ respectively, as τ is varied. As a result, the theoretical limit of the modulation frequency measurement is determined by the laser linewidth. In this case, the precision of using FPBCTS to measure $\Omega_2 - \Omega_1$ is determined by how well ω_1 and ω_2 can be tuned to the resonant frequencies of the transitions from $|0\rangle$ to $|1\rangle$ and from $|1\rangle$ to $|2\rangle$, respectively. In other words, we can obtain beating between the resonant frequencies of a cascade three-level system. The overall accuracy for the energy-level difference measurement is determined by the homogeneous linewidths of the optical transitions. Then a Doppler-free precision can be achieved in the measurement of $\Omega_2 - \Omega_1$. Equations (1) and (2) are different from the third-order beat signal intensity from channels (a)–(e).[2,3]

We then consider the case that beams 1 and 2 are broadband so that $\alpha_1 \gg \Gamma_{10}$ and $\alpha_2 \gg \Gamma_{20}$. In this case, the beat signal rises to its maximum quickly and then decays with a time constant mainly determined by the transverse relaxation times of the system. Although the beat signal modulation is complicated in general, at the tail of the signal (i.e., $\tau \gg \alpha_1^{-1}$, $\tau \gg \alpha_2^{-1}$) the beat signal intensity is: In the first beating approach, the beat signal intensity then becomes

$$\begin{aligned} I(\tau) \propto\ & |B_1'|^2 \exp[-4\Gamma_{10}|\tau|] \\ & + |\eta B_2'|^2 \exp[-2(\Gamma_{10} + \Gamma_{21})|\tau|] \\ & + \exp[-(3\Gamma_{10} + \Gamma_{21})|\tau|] \\ & \cdot \{B_1'^* \eta B_2' \exp[-\mathrm{i}\Delta\boldsymbol{k}\cdot\boldsymbol{r} - \mathrm{i}(\Omega_2 - \Omega_1)\tau] \\ & + B_1' \eta^* B_2'^* \exp[\mathrm{i}\Delta\boldsymbol{k}\cdot\boldsymbol{r} + \mathrm{i}(\Omega_2 - \Omega_1)\tau]\}. \end{aligned} \quad (3)$$

In the second beating approach, the beat signal intensity then becomes:

(i) for $\tau > 0$,

$$\begin{aligned} I(\tau) \propto\ & |B_2'|^2 \exp[-2(\Gamma_{10} + \Gamma_{21})|\tau|] \\ & + |\eta B_3'|^2 \exp[-4\Gamma_{20}|\tau|] \\ & + \exp[-(\Gamma_{10} + \Gamma_{21} + 2\Gamma_{20})|\tau|] \\ & \cdot \{B_2'^* \eta B_3' \exp[-\mathrm{i}\Delta\boldsymbol{k}\cdot\boldsymbol{r} - \mathrm{i}(\Omega_2 - \Omega_1)\tau - 2\mathrm{i}\Delta_1\tau] \\ & + B_2' \eta^* B_3'^* \exp[\mathrm{i}\Delta\boldsymbol{k}\cdot\boldsymbol{r} + \mathrm{i}(\Omega_2 - \Omega_1)\tau + 2\mathrm{i}\Delta_1\tau]\}. \end{aligned} \quad (4)$$

(ii) for

$$\tau < 0, I(\tau) \propto |B_2'|^2 \exp[-2(\Gamma_{10} + \Gamma_{21})|\tau|]. \quad (5)$$

Here B_1', B_2' and B_3' are τ-independent constants. Equations (3) and (4) indicate that the modulation frequency of the beat signal equals $\Omega_2 - \Omega_1$ when $\Delta_1 = 0$. Therefore, the modulation frequency, which corresponds directly to the beating between the resonant frequencies of a cascade three-level system, can be measured with accuracy given by $\pi(3\Gamma_{10} + \Gamma_{21})$ or $\pi(\Gamma_{10} + \Gamma_{21} + 2\Gamma_{20})$ approximately. In other words, the overall accuracy of using FPBCTS with broadband light to measure the energy-level difference between two states is limited by the homogeneous linewidths. On the other hand, Eqs.(3) and (4) are also different from the third-order beat signal intensity from channels (a)–(e).[2,3]

III. FPBCTS IN A DOPPLER-BROADENED SYSTEM

The beat signal can be calculated from a different viewpoint. In the Doppler-broadened limit (i.e., $k_3 u \to \infty$), we first consider the case that beams 1 and 2 are narrow bands so that $\alpha_1 \ll \Gamma_{10}$ and $\alpha_2 \ll \Gamma_{20}$. In the first beating approach, the beat signal intensity then becomes

$$\begin{aligned} I(\tau) \propto\ & |B_4|^2 \exp(-4\alpha_1|\tau|) \\ & + |\eta B_5|^2 \exp[-2(\alpha_1 + \alpha_2)|\tau|] \\ & + \exp[-(3\alpha_1 + \alpha_2)|\tau|] \\ & \cdot \{\eta B_4^* B_5 \exp[-\mathrm{i}\Delta\boldsymbol{k}\cdot\boldsymbol{r} - \mathrm{i}(\omega_2 - \omega_1)\tau] \\ & + \eta^* B_4 B_5^* \exp[\mathrm{i}\Delta\boldsymbol{k}\cdot\boldsymbol{r} + \mathrm{i}(\omega_2 - \omega_1)\tau]\}. \end{aligned} \quad (6)$$

In the second beating approach, the beat signal intensity then becomes

$$\begin{aligned} I(\tau) \propto\ & |B_5|^2 \exp[-2(\alpha_1 + \alpha_2)|\tau|] \\ & + |\eta B_6|^2 \exp(-4\alpha_2|\tau|) \\ & + \exp[-(\alpha_1 + 3\alpha_2)|\tau|] \\ & \cdot \{\eta B_5^* B_6 \exp[-\mathrm{i}\Delta\boldsymbol{k}\cdot\boldsymbol{r} - \mathrm{i}(\omega_2 - \omega_1)\tau] \\ & + \eta^* B_5 B_6^* \exp[\mathrm{i}\Delta\boldsymbol{k}\cdot\boldsymbol{r} + \mathrm{i}(\omega_2 - \omega_1)\tau]\}. \end{aligned} \quad (7)$$

Here B_4, B_5 and B_6 are τ-independent constants; $\Gamma_{10}^a = \Gamma_{10} + \xi_1\Gamma_{10}, \Gamma_{21}^a = \Gamma_{21} + \xi_2\Gamma_{10}, \Gamma_{20}^a = \Gamma_{20} + (\xi_2 - 1)\Gamma_{10}$; $\xi_1 = k_2/k_1, \xi_2 = k_3/k_1 > 1$.
Equations (6) and (7) are consistent with Eqs.(1) and (2), respectively.

We then consider the case that beams 1 and 2 are broad bands so that $\alpha_1 \gg \Gamma_{20}$ and $\alpha_2 \gg \Gamma_{20}$. In this case, the beat signal rises to its maximum quickly and then decays with a time constant mainly determined by the transverse relaxation time of the system. Although the beat signal modulation is complicated in general, at the tail of the signal (i.e., $\tau \gg \alpha_1^{-1}$, $\tau \gg \alpha_2^{-1}$) the beat signal intensity is:
(i) For $\tau > 0$
In the first beating approach, the beat signal intensity then becomes

$$\begin{aligned} I(\tau) \propto & |q_1|^2 \exp[-4\Gamma_{10}^a|\tau|] \\ & + |\eta q_2|^2 \times \exp[-2(\Gamma_{10}^a + \Gamma_{21}^a)|\tau|] \\ & + \exp[-(3\Gamma_{10}^a + \Gamma_{21}^a)|\tau|] \\ & \cdot \{q_1^* \eta q_2 \exp[-\mathrm{i}\Delta\boldsymbol{k}\cdot\boldsymbol{r} - \mathrm{i}(\Omega_2 - \Omega_1)\tau \\ & - \mathrm{i}(\xi_2 - \xi_1)\Delta_3\tau] \\ & + q_1\eta^* q_2^* \exp[\mathrm{i}\Delta\boldsymbol{k}\cdot\boldsymbol{r} + \mathrm{i}(\Omega_2 - \Omega_1)\tau \\ & + \mathrm{i}(\xi_2 - \xi_1)\Delta_3\tau]\}. \end{aligned} \tag{8}$$

In the second beating approach, the beat signal intensity then becomes

$$\begin{aligned} I(\tau) \propto & |q_2|^2 \exp[-2(\Gamma_{10}^a + \Gamma_{21}^a)|\tau|] \\ & + |\eta q_3|^2 \times \exp[-4\Gamma_{21}^a|\tau|] \\ & + \exp[-(\Gamma_{10}^a + 3\Gamma_{21}^a)|\tau|] \\ & \cdot \{q_2^* \eta q_3 \exp[-\mathrm{i}\Delta\boldsymbol{k}\cdot\boldsymbol{r} - \mathrm{i}(\Omega_2 - \Omega_1)\tau \\ & - \mathrm{i}(\xi_2 - \xi_1)\Delta_3\tau] \\ & + q_2\eta^* q_3^* \exp[\mathrm{i}\Delta\boldsymbol{k}\cdot\boldsymbol{r} + \mathrm{i}(\Omega_2 - \Omega_1)\tau \\ & + \mathrm{i}(\xi_2 - \xi_1)\Delta_3\tau]\}. \end{aligned} \tag{9}$$

Here q_1, q_2 and q_3 are τ-independent constants.
Equations (8) and (9) indicate that the modulation frequency of the beat signal equals $\Omega_2 - \Omega_1$ when $\Delta_3 = 0$. Therefore the modulation frequency, which corresponds directly to the beating between the resonant frequencies of a cascade three-level system, can be measured with accuracy given by $\pi(3\Gamma_{10}^a + \Gamma_{21}^a)$ or $\pi(\Gamma_{10}^a + 3\Gamma_{21}^a)$ approximately. In other words, the overall accuracy of using FPBCTS with broadband light to measure the energy-level difference between two states is limited by the homogeneous linewidths. Physically, Eqs.(8) and (9) are analogous to Eqs.(3) and (4), respectively.

(ii) For $\tau < 0$
In the first beating approach, the beat signal intensity then becomes

$$\begin{aligned} I(\tau) \propto & |C_1|^2 \exp(-4\alpha_1|\tau|) \\ & + |\eta C_2|^2 \exp[-2(\alpha_1 + \alpha_2)|\tau|] \\ & + \exp[-(3\alpha_1 + \alpha_2)|\tau|] \\ & \cdot \{\eta C_1^* C_2 \exp[-\mathrm{i}\Delta\boldsymbol{k}\cdot\boldsymbol{r} - \mathrm{i}(\omega_2 - \omega_1)\tau] \\ & + \eta^* C_1 C_2^* \exp[\mathrm{i}\Delta\boldsymbol{k}\cdot\boldsymbol{r} + \mathrm{i}(\omega_2 - \omega_1)\tau]\}. \end{aligned} \tag{10}$$

In the second beating approach, the beat signal intensity then becomes

$$\begin{aligned} I(\tau) \propto & |C_2|^2 \exp[-2(\alpha_1 + \alpha_2)|\tau|] \\ & + |\eta C_3|^2 \exp(-4\alpha_2)|\tau|) \\ & + \exp[-(\alpha_1 + 3\alpha_2)|\tau|] \\ & \cdot \{\eta C_2^* C_3 \exp[-\mathrm{i}\Delta\boldsymbol{k}\cdot\boldsymbol{r} - \mathrm{i}(\omega_2 - \omega_1)\tau] \\ & + \eta^* C_2 C_3^* \exp[\mathrm{i}\Delta\boldsymbol{k}\cdot\boldsymbol{r} + \mathrm{i}(\omega_2 - \omega_1)\tau]\}. \end{aligned} \tag{11}$$

Here C_1, C_2, and C_3 τ-independent constants. Equations (10) and (11) are consistent with Eqs.(1) and (2), respectively.

IV. PHOTON ECHO

It is interesting to understand the underlying physics in FPBCTS with incoherent lights. Much attention has been paid to the study of various ultrafast phenomena by using incoherent light sources recently.[18−20] Under the phase matching condition $2\boldsymbol{k}_1 - 2\boldsymbol{k}_1' + \boldsymbol{k}_3$, the three-pulse stimulated photon echoes exist for the perturbation chains (I) and (II). Under the phase matching conditions $2\boldsymbol{k}_2 - 2\boldsymbol{k}_2' + \boldsymbol{k}_3$ and $\boldsymbol{k}_3 + \boldsymbol{k}_1 - \boldsymbol{k}_1' + \boldsymbol{k}_2 - \boldsymbol{k}_2'$, the sum-frequency trilevel echoes exist for the perturbation chains (III)–(V).[19] In the Doppler-broadened limit (i.e., $k_3 u \to \infty$), we consider the case that beams 1 and 2 are broadband. Then $< u_i(t_1)u_i^*(t_2) >= \exp(-\alpha_i|t_1 - t_2|) \approx \frac{2}{\alpha_i}\delta(t_1 - t_2)$, i=1, 2. Photon echo does not exist for the perturbation chains (VI).

(i) For $\tau > 0$, the fifth-order beat signal intensity from channels (I), (II), (III), (V) is

$$\begin{aligned} I(\tau) \propto & | < P^{(5)} > |^2 = |q_1'|^2 \exp[-4\Gamma_{10}^a|\tau|] \\ & + |\eta q_2'|^2 \exp[-2(\Gamma_{10}^a + \Gamma_{21}^a)|\tau|] \\ & + \exp[-(3\Gamma_{10}^a + \Gamma_{21}^a)|\tau|] \\ & \cdot \{q_1'^* \eta q_2' \exp[-\mathrm{i}\Delta\boldsymbol{k}\cdot\boldsymbol{r} \\ & - \mathrm{i}(\Omega_2 - \Omega_1)\tau - \mathrm{i}(\xi_2 - \xi_1)\Delta_3\tau] \\ & + q_1'\eta^* q_2'^* \exp[\mathrm{i}\Delta\boldsymbol{k}\cdot\boldsymbol{r} + \mathrm{i}(\Omega_2 - \Omega_1)\tau \\ & + \mathrm{i}(\xi_2 - \xi_1)\Delta_3\tau]\}. \end{aligned} \tag{12}$$

The fifth-order beat signal intensity from channels (III)–(V) becomes

$$\begin{aligned} I(\tau) \propto & |q_2'|^2 \exp[-2(\Gamma_{10}^a + \Gamma_{21}^a)|\tau|] \\ & + |\eta q_3'|^2 \exp[-4\Gamma_{20}^a|\tau|] \\ & + \exp[-(\Gamma_{10}^a + \Gamma_{21}^a + 2\Gamma_{20}^a)|\tau|] \\ & \cdot \{q_2'^* \eta q_3' \exp[-\mathrm{i}\Delta\boldsymbol{k}\cdot\boldsymbol{r} \\ & - \mathrm{i}(\Omega_2 - \Omega_1)\tau - \mathrm{i}(\xi_2 - \xi_1)\Delta_3\tau] \\ & + q_2'\eta^* q_3'^* \exp[\mathrm{i}\Delta\boldsymbol{k}\cdot\boldsymbol{r} \\ & + \mathrm{i}(\Omega_2 - \Omega_1)\tau + \mathrm{i}(\xi_2 - \xi_1)\Delta_3\tau]\}. \end{aligned} \quad (13)$$

Here q_1', q_2' and q_3' are τ-independent constants. Equations (12) and (13) are consistent with Eqs.(3) and (4), respectively.

(ii) For $\tau < 0$, photon echoes do not exist for the perturbation chains (I)–(V). The requirement for the existence of a τ-dependent beat signal for $\tau < 0$ is that the phase-correlated subpulses in beams 1 and 2 are overlapped temporally. Since beams 1 and 2 are mutually coherent, the temporal behaviour of the beat signal should coincide with the case when the beams 1 and 2 are nearly monochromatic. Therefore, these cases are also consistent with Eqs.(1) and (2).

V. DISCUSSION AND CONCLUSION

FPBCTS can be considered as a technique which possesses the main features of the high resolution laser spectroscopies in the frequency and time domains. Firstly, FPBCTS is closely related to the Doppler-free saturated absorption spectroscopy and two-photon absorption spectroscopy in tuning ω_1 and ω_2 to the resonant frequencies when narrow-band lights are used. However, unlike the techniques in the frequency domain, here we are interested in the temporal behaviour of the signal, and the frequencies of the laser do not need to be calibrated. In this sense FPBCTS is similar to the spectroscopies in the time domain. FPBCTS is related intrinsically to the optical coherent transient spectroscopy when broadband lights are used. In these cases, when pulse laser beams 1 and 2 are separated temporally, then before the application of beam 2, the polarization exhibits free evolution. As a result, the modulation frequency is directly related to the energy level of the system, no matter whether the beams have a narrow-band or broadband linewidth. The advantage of FPBCTS over other time-domain techniques is that the temporal resolution is not limited by the laser pulse width.

However, for highly nonlinear media such as semiconductor, polymers and some special glasses, high-order nonlinearities may also contribute even at moderate intensity levels. In principle, the interference effect may be observed in a large variety of materials, and the exploitation of this phenomenon to develop a new technique for nonlinear spectroscopy is also discussed.[4] The signal modulation depth is dependent on the ratio $\chi^{(5)}/\chi^{(3)}$ and can be adjusted by changing the laser relative intensities,[5,16] where $\chi^{(3)}$ and $\chi^{(5)}$ are the third- and fifth-order susceptibilities, respectively. Based on Eq.(1), we have calculated the FPBCTS in sodium vapour, where the ground state $3S_{1/2}$, the intermediate state $3P_{3/2}$ and the excited state $4D_{3/2,5/2}$ formed a cascade three-level system. Figure 3 presents the temporal behaviour of the normalized beat signal intensity versus relative time delay. Parameters used are α_1=2.7 ps^{-1}, α_2=2.9 ps^{-1}, λ_1=589.0 nm, λ_2=568.8 nm, $\Delta k = 0$ and η=B_1=B_2=1. It shows that as τ varies, the beat signal intensity modulates sinusoidally with period 55 fs. Figure 4 shows the Fourier spectrum of the data, in which τ is varied over a range of 2.0 ps. Then we obtain the modulation frequency 114 ps^{-1}, corresponding to the beating between the resonant frequencies of the transitions from $3S_{1/2}$ to $3P_{3/2}$ and from $3P_{3/2}$ to $4D_{3/2,5/2}$. The modulation frequency can be obtained

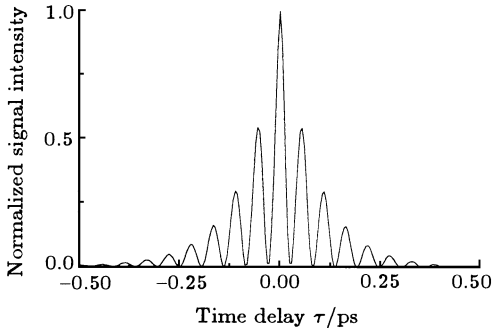


Fig.3. Normalized beat signal intensity versus relative time delay. Parameters are α_1=2.7 ps^{-1}, α_2=2.9 ps^{-1}, λ_1=589.0nm, λ_2=568.8nm, $\Delta k = 0$ and η=B_1=B_2=1.

more directly by making a Fourier transformation of the FPBCTS data. Figure 5 presents the spatial behaviour of normalized polarization beat signal intensity versus transverse distance r. Parameters used are α_1=2.7 ps^{-1}, α_2=2.9 ps^{-1}, τ=1 ps, $\theta = 2.62 \times 10^2$rad, λ_1=589.0nm, λ_2=568.8nm and η=B_1=B_2=1.

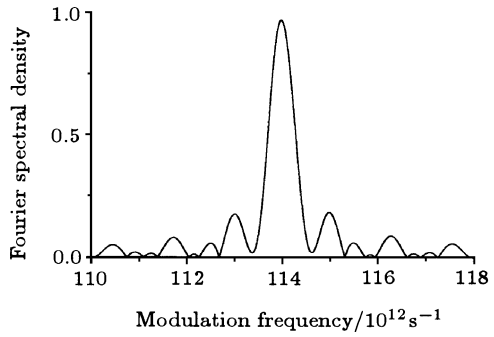


Fig.4. Fourier spectrum of the FPBCTS data in which τ is varied over a range of 2.0 ps.

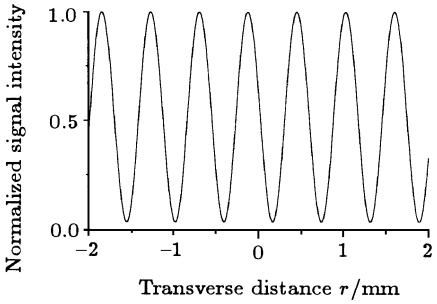


Fig.5. Normalized polarization beat signal intensity versus transverse distance r. Parameters are α_1=2.7 ps^{-1}, α_2=2.9 ps^{-1}, τ=1 ps, $\theta = 2.62 \times 10^{-2}$ rad, λ_1=589.0 nm, λ_2=568.8 nm and η=B_1=B_2=1.

In conclusion, we have studied theoretically a phase-conjugate ultrafast modulation spectroscopy due to the interference between fifth- and fifth-order optical polarizations in a cascade three-level Doppler-broadened system. It is found that the temporal behaviour of the beat signal depends on the stochastic properties of the lasers and the transverse relaxation rate of the atomic energy-level system. The beat signal depends on the second-order coherence function, which is determined by the laser lineshape. Since different stochastic models of the laser field only affect higher than second-order coherence functions, they have little influence on the general temporal modulation behaviour of the beat signal. We have considered the cases that pump beams have either narrowband or broadband linewidth and found that for both cases a Doppler-free precision in the measurement of the energy-level difference between two states can be achieved. The advantage of FPBCTS is that the energy-level difference between states can be widely separated. It is worth mentioning that the asymmetric behaviour of the polarization beat signal, which is due to the dispersion of the optical components in a cascade three-level system, do not affect the overall accuracy of using FPBCTS to measure the energy-level difference.[21,22] Furthermore, FPBCTS can tolerate small perturbations of the optical path due to mechanical vibration and distortion of the optical components, as long as these are small compared with $c/|\omega_2 - \omega_1|$.

References

[1] DeBeer D, Van Wagenen L G, Beach R and Hartmann S R 1986 *Phys. Rev. Lett.* **56** 1128

[2] Fu P M, Yu Z H, Mi X, Li X F and Jiang Q 1994 *Phys. Rev.* A **50** 698

[3] Zhang Y P, Tang T T, Sun L Q and Fu P M 2000 *Phys. Rev.* A **61** 023809

[4] Ma H, Acioli L H, Gomes A S L and de Araujo C B 1991 *Opt. Lett.* **16** 630

[5] Ma H and de Araujo C B 1993 *Phys. Rev. Lett.* **71** 3649

[6] Elliott S, Hamilton M W, Arnett K and Smith S J 1984 *Phys. Rev. Lett.* **53** 439

[7] Zhang Y P, Wu H C, Wang P F, Li C S and Fu P M 2000 *Chin. Phys.* **9** 599

[8] Do B, Cha J, Elliott D S and Smith S J 1999 *Phys. Rev.* A **60** 508

[9] Zhang Y P, Tang T T and Fu P M 1999 *Acta Phys. Sin.* **48** 242

[10] Zhang Y P, Sun L Q, Tang T T and Fu P M 2000 *J. Opt. Soc. Am.* B **17** 690

[11] Zhang Y P, Sun L Q, Tang T T, Zhang L and Fu P M 2000 *Chin. Phys. Lett.* **17** 206

[12] Zhang Y P, Lu K Q, Wu H C, Xu J and Fu P M 2000 *Chin. Phys.* **9** 606

[13] Chen C, Elliott D S and Hamilton M W 1992 *Phys. Rev. Lett.* **68** 3531

[14] Walser R, Ritsch H, Zoller P and Cooper J 1992 *Phys. Rev.* A **45** 468

[15] Anderson M H, Vemuri G, Cooper J, Zoller P and Smith S J 1993 *Phys. Rev.* A **47** 3202

[16] Ulness D J, Kirkwood J C and Albrecht A C 1998 *J. Chem. Phys.* **108** 3897

[17] Zhang Y P, Hou X, Lu K Q and Wu H C 2000 *Opt. Commun.* **184** 265

[18] Morita N and Yajima T 1984 *Phys. Rev.* A **30** 2525

[19] Zhang Y P, Gan C L, Zhu J P, Tang T T and Fu P M 1999 *Acta Phys. Sin.* **48** 1667

[20] Zhang Y P, Tang T T, Li S and Sun L Q 1999 *Acta Phys. Sin.* **48** 1452

[21] Zhang Y P, Sun L Q, Tang T T and Fu P M 2000 *Phys. Rev.* A **61** 053819

[22] Fu P M, Mi X, Yu Z H, Jiang Q, Zhang Y P and Li X F 1995 *Phys. Rev.* A **52** 4867